2011 Switzerland
reviewed 7/2022
evidence that iron and iodine accumulate in the liver!

Quantification of Liver Fat in the Presence of Iron and Iodine

An Ex-Vivo Dual-Energy CT Study

Michael A. Fischer, MD, Ralph Gnannt, MD,* Dimitri Raptis, MD,† Caecilia S. Reiner, MD,* Pierre-Alain Clavien, MD,† Bernhard Schmidt, PhD,‡ Sebastian Leschka, MD,§ Hatem Alkadhi, MD, MPH,* and Robert Goetti, MD**

Purpose: Iodinated contrast media (CM) and iron in the liver are known to hinder an accurate quantification of liver fat content (LFC) with single-energy computed tomography (SECT). The purpose of this study was to evaluate the feasibility and accuracy of dual-energy CT (DECT) for ex vivo quantification of LFC, in the presence of iron and CM, compared with SECT.

Materials and Methods: Sixteen phantoms with a defined LFC of 0%, 10%, 30%, and 50% fat and with varying iron content (0, 1.5, 3, and 6 mg/mL wet weight liver) were scanned with a second-generation dual-source 128-slice CT system. Phantoms were scanned unenhanced and contrast-enhanced after adding 1.0 mg/mL iodine to each phantom. Both SECT (120 kV) and DECT (tube A: 140 kV, using a tin filter 228 mAs; tube B: 80 kV, 421 mAs) data were acquired. An iron-specific dual-energy 3-material decomposition algorithm providing virtual noniron images (VNI) was used to subtract iron and CM from the data. CT numbers (Hounsfield units) were measured in all data sets, including 120 kV from SECT, as well as 140 kV, 80 kV, 50%:50% weighted 80 kV/140 kV, and VNI derived from DECT. The dual-energy index was calculated from 80 kV and 140 kV data. SECT and DECT measurements (Hounsfield units) including the dual-energy index of unenhanced and contrast-enhanced phantoms were compared with the known titrated LFC, using Pearson correlation analysis and Student *t* test for related samples.

Results: Inter-reader agreement was excellent for all measurements of CT numbers in both SECT and DECT data (Pearson *r*, 0.965–1.0). For fat quantification in the absence of iron and CM, CT numbers were similar in SECT and DECT (all, $P > 0.05$), showing a linear correlation with titrated LFC (*r* ranging from 0.981 to 0.999; $P < 0.01$). For fat quantification in the presence of iron but without CM, significant underestimation of LFC was observed for all measurements in SECT and DECT ($P < 0.05$), except for VNI. Measurements in VNI images allowed for an accurate LFC estimation, with no significant differences compared with measurements in iron-free phantoms (all, $P > 0.25$). For fat quantification in the presence of iron and CM, further underestimation of LFC was seen for measurements in SECT and DECT ($P < 0.015$), except for VNI. Measurements in VNI images showed a high accuracy for estimating the LFC, with no significant difference compared with measurements in iron- and CM-free phantoms ($P > 0.2$).

Conclusions: Our ex vivo phantom study indicates that DECT with the use of a dedicated, iron-specific 3-material decomposition algorithm allows for the accurate quantification of LFC, even in the presence of iron and iodinated CM. VNI images reconstructed from DECT data equal nonenhanced SECT data of liver without CM by eliminating iron and iodine from the images. No added value was seen for DECT as compared with SECT for quantification of LFC in the absence of iron and iodine.

Key Words: liver fat content, iron, contrast media, computed tomography, dual-energy

(*Invest Radiol* 2011;46: 351–358)

Hepatic steatosis, defined as elevated triglyceride content of the liver, has many underlying causes, including alcohol, metabolic diseases, and nutritional disorders.[1] As a consequence of the metabolic syndrome, the prevalence of hepatic steatosis has markedly increased in the past years and has been estimated to affect 13% to 23% of the Western population.[2,3] Early diagnosis and treatment of both alcoholic and nonalcoholic hepatic steatosis are important due to their potential to progress to end-stage liver disease. In addition, fatty liver has a lower regeneration potential, affecting the outcomes of both conservative therapy and liver surgery.[4,5] Therefore, accurate quantification of liver fat content (LFC) is of major clinical interest for the primary evaluation of diffuse liver disease as well as for monitoring treatment response.[6]

To date, liver biopsy with sampling of histopathology represents the reference standard method for the quantification of LFC. However, the method is invasive, is subject to sampling errors, and histopathology is known to suffer from a considerable inter-reader variability.[7,8] Among the noninvasive methods of LFC quantification, magnetic resonance (MR) imaging and especially MR spectroscopy has gained an important role in providing accurate measures of LFC.[9,10] However, limited availability of MR spectroscopy and the dependence of fat measurements with MR imaging on protocol parameters as well as local field inhomogeneity preclude a widespread use of MR for the evaluation of hepatic steatosis.[10,11]

In clinical practice, computed tomography (CT) is commonly used for the imaging evaluation of chronic hepatic disease. The degree of fat deposition can be estimated based on the hepatic attenuation reflected by a decrease in Hounsfield units (HU) with increasing LFC. In the presence of iron and contrast media (CM), however, quantification of LFC is no longer possible with single-energy CT (SECT).[12] Both iron and CM confound measurements by increasing attenuation with higher iron and/or iodine concentrations, an inverse effect to fat.[13,14] This issue is of major clinical concern because iron often coexists with fat depositions in chronic, diffuse liver disease. For example, alcoholic liver disease, which is characterized by fatty liver, fibrosis, hepatitis, and cirrhosis, usually is associated with mild-to-severe iron overload.[15] Moreover, quantification of LFC would be desirable also in CM-enhanced CT studies of the liver.

Dual-source CT, being equipped with 2 x-ray tubes and 2 corresponding detector units, enables the simultaneous acquisition of data with 2 different tube voltages. The resulting dual-energy CT (DECT) data allows distinguishing materials with comparable atomic numbers due to differences in the photo and Compton effect on CT attenuation at different photon energies.[16] Accordingly,

Received September 21, 2010; accepted for publication (after revision) December 31, 2010.

From the *Institute of Diagnostic and Interventional Radiology, University Hospital Zurich, Zurich, Switzerland; †Clinic of Visceral and Transplant Surgery, University Hospital Zurich, Zurich, Switzerland; ‡Imaging and IT Division, Siemens Healthcare, Forchheim, Germany; and §Institute of Radiology, General Hospital Saint Gall, Saint Gall, Switzerland.

Reprints: Hatem Alkadhi, MD, MPH, Institute of Diagnostic and Interventional Radiology, University Hospital Zurich, Raemistr 100, 8091 Saint Gall, Switzerland. E-mail: hatem.alkadhi@usz.ch.

ISSN: 0020-9996/11/4606-0351

DECT was shown able to accurately predict the liver iron content (LIC) in an animal study.[17] DECT has been recently further improved by introducing a tin filter, which improves the separation of the 2 energy spectra and thus, the ability to differentiate and characterize different body materials.[18,19]

The purpose of this study was to evaluate the feasibility and accuracy of DECT for the ex vivo quantification of LFC in the presence of iron and CM, compared with SECT.

MATERIALS AND METHODS

Phantoms

Sixteen 15 mL polypropylene test tubes (FALCON, Becton Dickinson and Co., NJ) containing 10 mL of homogenized mixtures of liver tissue (veal liver), titrated fat (goose fat), and iron (iron-chloride) were placed in a grid and were submerged in a 22 × 30 × 40 cm^3 tank filled with distilled water, simulating body attenuation.

Liver/fat mixtures, using fat concentrations of 0%, 10%, 30%, and 50% were prepared 4 times to allow for adding iron (Fe^{3+}) in 4 different concentrations.

The following iron concentrations were used: 0 mg/mL wet-liver simulating healthy liver, 1.5 mg/mL wet-liver simulating slightly elevated LIC, and 3 and 6 mg/mL wet-liver simulating mild and severe hemosiderosis, respectively.[20] For conversion of LIC of dry-liver reported in the literature to LIC of wet-liver used for phantom preparation, a conversion factor of 1/3.33 was applied, as previously shown.[21]

The phantom position in the grid was noted by one radiologist not involved in further CT data analysis, and phantoms were scanned according to the imaging protocol described below.

After scanning of the "nonenhanced" phantoms, iodine containing CM (iopromide, Ultravist 300, 300 mg/mL, Bayer Schering Pharma, Berlin, Germany) at a concentration of 1 mg/mL was added to all 16 test tubes, which were homogenized and scanned again using the same grid position and scan protocol.

DECT Data Acquisition

All CT scans were performed using a dual-source 128-slice CT system (SOMATOM Definition Flash, Siemens Healthcare, Forchheim, Germany) equipped with a tin filter for improved separation of the 2 energy spectra.[18] First, single-energy images were acquired using a tube voltage of 120 kV and a tube current-time product of 210 mAs per rotation (effective tube current-time product, 410 mAs; CT dose index [CTDIvol], 2.01 mGy). Further scanning parameters were: detector collimation of 64 × 0.6 mm^2, slice acquisition of 128 × 0.6 mm^2 using a flying focus along the z-axis with 2 different focal spots, gantry rotation time of 500 milliseconds, and pitch 0.6. Then, dual-energy images were acquired using a tube voltage pair of 140 kV and 80 kV and a tube current-time product pair of 192 mAs per rotation (effective, 384 mAs) and 497 mAs per rotation (effective, 994 mAs), respectively, while keeping all other parameters unchanged as for the SECT data acquisition. CTDIvol for this setting was 2.88 mGy.

All DECT images were reconstructed with a slice thickness of 1.5 mm and an increment of 1 mm, using a dedicated dual-energy kernel (D30f). SECT images were reconstructed with the same slice thickness and increment, using a standard medium-smooth soft-tissue kernel (B30f).

DECT Image Reconstruction

All images were reconstructed by 1 radiologist who was not involved in the CT data analysis.

For each phantom, the following 5 sets of images were reconstructed:

1. Single-energy images acquired at 120 kV (SE_{120}),
2. 80 kV images acquired during DECT (DE_{80}),
3. 140 kV images acquired during DECT (DE_{140}),
4. Linearly blended images using a 50%:50% weighted ratio of the 80 kV and 140 kV dual-energy data ($DE_{80/140}$), and
5. Virtual noniron (VNI) images derived from dual-energy 3-material decomposition, using DECT data acquired at 80 kV and 140 kV (Fig. 1).

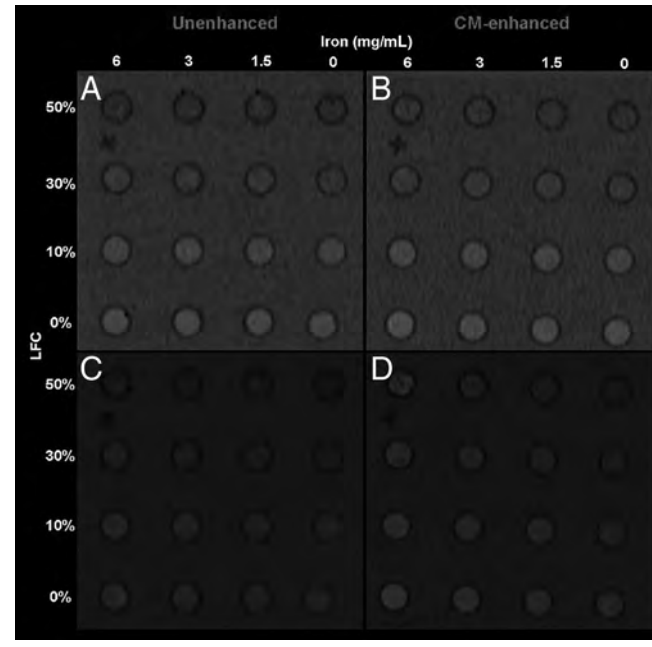

FIGURE 1. Dual-energy 3-material decomposition of fat, liver tissue, and high atomic number material: red overlay images (C, D) reflect content of high atomic number material (iron [C] and iodine plus iron [D]), which was subtracted from the computed tomography (CT) images to produce virtual noniron images (VNI) (A, B).

Dual-energy 3-material decomposition was used in this study to differentiate fat, liver tissue, and iron, by using commercially available postprocessing software ("Liver virtual non-contrast [VNC]," *syngo* Dual Energy, Siemens AG, Forchheim, Germany). Briefly, the sum of masses of the 3 constituent materials is equivalent to the mass of the mixture. With this assumption it is possible to solve an equation for 3 unknown variables with only 2 spectral measurements, using a mass-conservation based, 3-material decomposition DECT algorithm.[22] Presettings of this algorithm are optimized for the decomposition of iodine but can be adjusted for any high atomic number material (such as iron). To subtract iron from the CT data, an iron-specific algorithm was generated as follows:

First, both the liver component as well as the fat component used for the phantom preparation were calibrated for 80 kV and 140 kV, using samples of 100% liver tissue and 100% fat; whereas, the "iron-specific" slope was derived from relative attenuation differences between 80 kV and 140 kV. Accordingly, the "iron-specific" slope of 2.9 is the ratio of the slopes at 80 kV (9.4) and 140 kV (3.2) determined using samples containing liver tissue and iron at concentrations of 1.5, 3, and 6 mg/mL (Fig. 2).

CT Data Analysis

Two independent and blinded radiologists (with 3 and 4 years of experience in abdominal radiology, respectively) measured CT numbers on 3-mm thick reformations of all image sets from all phantoms. Measurements were performed in random order by plac-

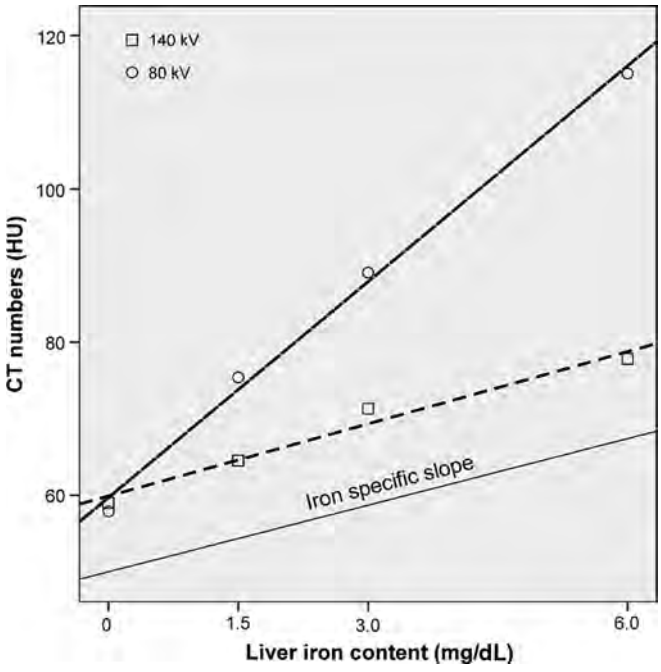

FIGURE 2. Single-energy CT (SECT) number measurements at 80 kV and 140 kV at iron concentrations of 0 mg/mL, 1.5 mg/mL, 3 mg/mL, and 6 mg/mL. The "iron-specific" slope of 2.9 for dual-energy 3-material decomposition was derived from relative attenuation differences between 80 kV and 140 kV.

ing a region of interest covering the entire long-axis of the phantom, avoiding edges as to not include partial volume artifacts (mean size, 5.87 ± 0.23 cm^2).

Based on the CT attenuation measurements (in HU) derived from the 80 kV and 140 kV data, the dual-energy index (DEI) was calculated for each phantom as follows[23]:

$$\text{DEI} = (\text{CT numbers at 80 kV} - \text{CT numbers at 140 kV})/(\text{CT numbers at 80 kV} + \text{CT numbers at 140 kV} + 2000\ \text{HU})$$

Statistical Analysis

Variables are described as mean ± standard deviation or as percentages. The data was descriptively analyzed and statistically tested for normality using the Kolmogorov–Smirnov test.

Correlation between the measurements by both the readers were assessed by Pearson correlation analysis. The interobserver variability was assessed according to the method of Bland and Altman and was determined as the mean differences (bias) with corresponding limits of agreement. Because interobserver variability was minimal (see Results section), the mean of both measurements was taken for further analysis.

Correlation between CT measurements and titrated LFC as well as titrated LIC was assessed using Pearson correlation analysis. Student *t* test for related samples was used to test for significant differences between CT measurements of different groups of LIC and between CT measurements of unenhanced and contrast-enhanced phantoms. Estimated LFC from SECT and DECT data was determined using the method of least squares.

P values less than 0.05 were considered statistically significant. All statistical analyses were performed using commercially

TABLE 1. CT Numbers (HU) of Nonenhanced Phantoms With Different Fat and Iron Concentrations

Nonenhanced Phantom	Iron Free Fat Concentration				Iron Concentration		
	0%	10%	30%	50%	1.5 mg/mL Mean Increase (95% CI)*	3 mg/mL Mean Increase (95% CI)*	6 mg/mL Mean Increase (95% CI)*
120 kV	58.4	33.3	−5.3	−19.6	Δ13.2 (7.5 to 18.9, $P < 0.01$)	Δ27.2 (16.0 to 38.3, $P < 0.01$)	Δ43.6 (27.7 to 59.5, $P < 0.01$)
80 kV	58.2	35.8	−11	−28.2	Δ19.7 (13.7 to 25.6, $P < 0.01$)	Δ37.8 (24.7 to 50.8, $P < 0.01$)	Δ62.1 (44.3 to 79.8, $P < 0.01$)
140 kV	58.4	41.3	5.1	−7.8	Δ7.9 (3.9 to 11.9, $P < 0.01$)	Δ15.9 (5.9 to 26.1, $P < 0.05$)	Δ22.4 (8.4 to 36.3, $P < 0.05$)
$DE_{80/140}$	59.3	38	−2.2	−18.7	Δ14.7 (11.3 to 18.1, $P < 0.01$)	Δ27.5 (17.1 to 37.8, $P < 0.04$)	Δ41.4 (27.9 to 54.9, $P < 0.02$)
DEI	−0.0001	−0.0026	−0.0081	−0.0104	Δ0.0058 (0.0046 to 0.0069, $P < 0.001$)	Δ0.0106 (0.0083 to 0.0129, $P < 0.001$)	Δ0.0189 (0.0159 to 0.0219, $P < 0.001$)
VNI	57.9	35.7	−7.1	−19.7	Δ0.8 (−2.5 to 4.0, $P = 0.51^{\dagger}$)	Δ4.2 (−5.4 to 13.7, $P = 0.26^{\dagger}$)	Δ3.3 (−9.8 to 16.3, $P = 0.49^{\dagger}$)

*Mean differences of CT numbers for iron concentrations of 1.5 mg/mL and higher compared to the mean of iron-free phantoms are shown.
†Nonsignificant differences.
HU indicates Houndsfield units; $DE_{80/140}$, 50%:50% linearly blended images at 80 kV and 140 kV; DEI, dual-energy index; VNI, virtual noniron images; CI, confidence interval.

available software (Statistical Package for Social Sciences, release 17.0, Chicago, IL).

RESULTS

Inter-reader Agreement

Inter-reader agreement was excellent for all DECT and SECT measurements of nonenhanced phantoms without and with iron supplementation (Pearson *r*, 0.973–1.0 and 0.982 –1.0, respectively). Similar results were obtained for the contrast-enhanced phantoms (Pearson *r*, 0.979−0.999 and 0.965–1.0, respectively).

Mean measurement biases were low, ranging from −0.32 to 0.65 HU (limits of agreement, −2.86 to 3.43 HU) for nonenhanced CT without iron, from −0.50 to 0.76 HU (limits of agreement, −2.89 to 3.84 HU) for nonenhanced CT with iron, and from −0.92 to 0.51 HU (limits of agreement, −4.68 to 3.16 HU) for contrast-enhanced CT.

Because interobserver variability and biases were minimal, the mean of both measurements was taken for further analysis.

Fat Quantification in the Absence of Iron and Iodine

For iron-free, nonenhanced phantoms, with a defined LFC of 0%, 10%, 30%, and 50% fat, no significant differences were observed between SE_{120}, DE_{80}, DE_{140}, $DE_{80/140}$, and VNI (all, $P >$ 0.05), with CT attenuation numbers ranging between −28.2 and 59.3 HU (Table 1).

Significant linear correlation between CT attenuation and titrated LFC was observed for all 5 image sets (Fig. 3A), with Pearson correlation coefficients ranging from 0.981 to 0.999 (all, *P*

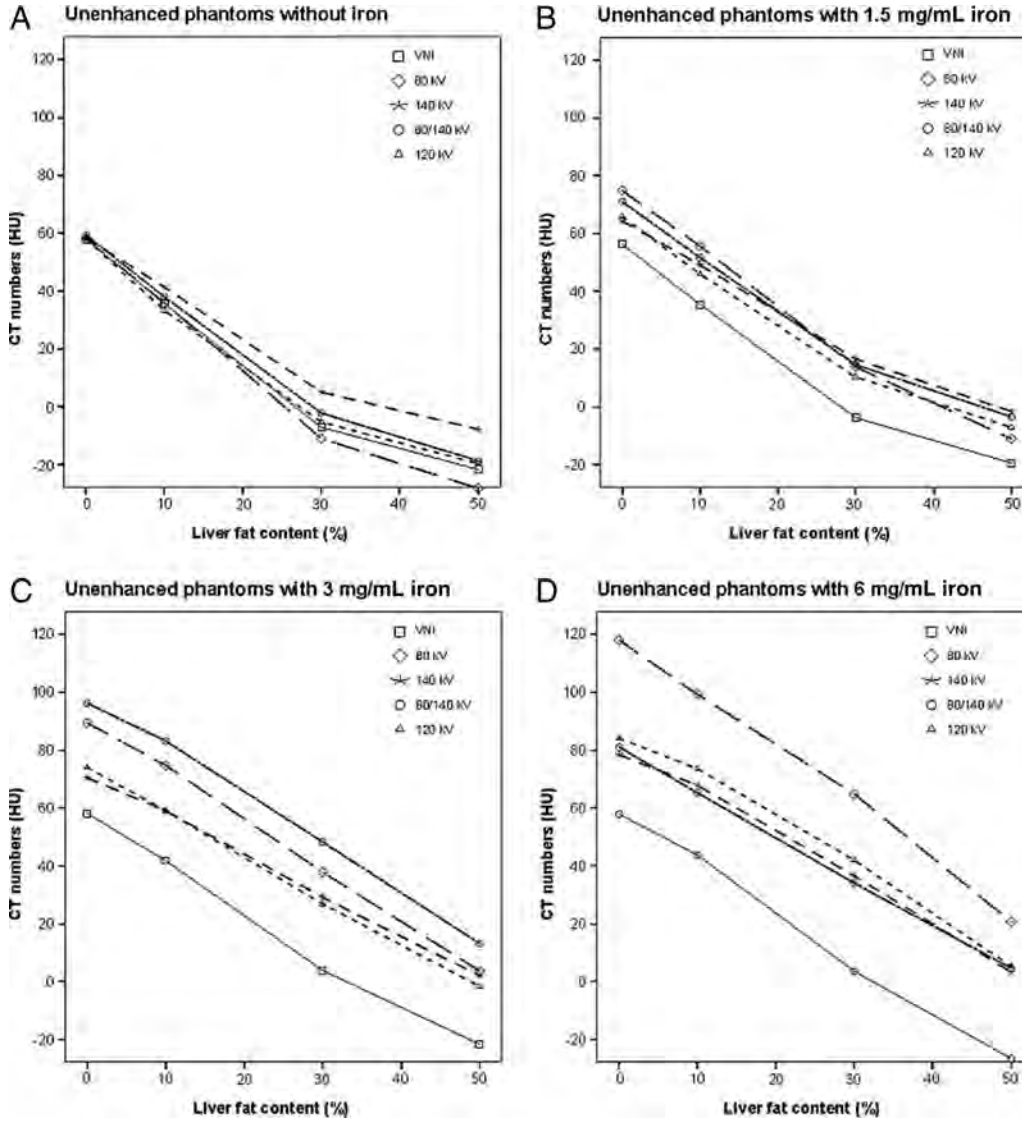

FIGURE 3. Comparison of CT measurements at 120 kV, 80 kV, 140 kV, and 80/140 kV with VNI measurements derived from dual-energy CT (DECT) for unenhanced (iodine free) phantoms. For unenhanced phantoms at 0 mg/mL iron (A) SECT and DECT including VNI numbers were similar showing no significant difference in fat quantification ($P > 0.05$). With increasing iron content (B–D) there was a significant underestimation of titrated liver fat content (LFC) for all measurements (all, $P <$ 0.05) except for VNI, which correctly estimated the LFC for low (B), medium (C), and high (D) iron concentration (all, $P >$ 0.25).

< 0.01). DEI measurements ranged from -0.0001 to -0.0104 (Table 1), also showing a significant linear correlation to titrated LFC ($r = 0.987$, $P < 0.001$).

Fat Quantification in the Presence of Iron Without Iodine

For iron-containing, nonenhanced phantoms with defined LFC of 0%, 10%, 30%, and 50% fat, significant underestimation of LFC was seen for SE_{120}, DE_{80}, DE_{140}, $DE_{80/140}$, and DEI, with increasing LIC, even at a low LIC of 1.5 mg/mL (all, $P < 0.015$). In contrast, no significant differences in CT numbers (HU) were seen for VNI images of phantoms with low ($P = 0.51$), medium ($P = 0.26$), and high ($P = 0.491$) LIC, as compared with iron-free phantoms (Table 1). This indicated that CT number measurements in VNI images from DECT allow for the quantification of titrated LFC, regardless of the LIC, by eliminating iron from the data (Figs. 3B–D).

Correlation of CT number measurements after iron supplementation remained linear for all 4 LIC reflected by a parallel shift of CT values within the coordinate system (Fig. 3). Pearson correlation coefficients for SE_{120}, DE_{80}, DE_{140}, $DE_{80/140}$, DEI, and VNI were similarly high, ranging from 0.954 to 1.0 (all, $P < 0.05$).

Fat Quantification in the Presence of Iron and Iodine

When adding 1.0 mg/mL iodine to iron-free phantoms with a defined LFC of 0%, 10%, 30%, and 50% fat, a significant underestimation of LFC was seen for SE_{120}, DE_{80}; DE_{140}, $DE_{80/140}$, and DEI (all, $P < 0.05$). In contrast, CT measurements in VNI images accurately estimated titrated LFC, with CT numbers being similar to unenhanced VNI measurements ($P = 0.071$) (Table 2).

Pearson correlation coefficients ranged from 0.992 to 0.999 ($P < 0.01$) for all CT measurements when comparing unenhanced with contrast-enhanced phantoms (Fig. 4A).

Comparable to unenhanced phantoms, there was a significant underestimation of LFC when adding iron to the contrast-enhanced phantoms even at a low LIC of 1.5 mg/mL (all, $P < 0.015$). Again, no significant differences were seen for measurements in VNI images in contrast-enhanced phantoms with low ($P = 0.27$), medium ($P = 0.33$), and high ($P = 0.20$) LIC, as compared with iron-free phantoms (Table 2). This indicates that attenuation measurements in VNI images from DECT allow for the accurate quantification of titrated LFC by eliminating iron and iodine from the data (Figs. 4B–D).

Correlation between SE_{120}, DE_{80}, DE_{140}, $DE_{80/140}$, and DEI measurements with defined LFC was linear and significant for all 4 LIC (Pearson r, 0.971–0.992 and 0.972–0.991, respectively; all, $P < 0.03$). Linear correlation was also shown for VNI measurements at zero to medium LIC (Pearson r, 0.978–0.991; $P < 0.02$). No significant correlation was seen for a high LIC of 6 mg/mL (Pearson $r = 0.959$, $P = 0.182$).

Figure 5 summarizes the main results of this study. In an unenhanced phantom and in the absence of iron, SECT and DECT are equally suitable for the estimation of LFC. However, both iron and CM confound LFC quantification in SECT by increasing the attenuation of the liver phantoms in contrast to the attenuation lowering effect of fat. VNI derived from DECT, on the other hand, is able to accurately quantify the titrated LFC by virtually eliminating iron and iodine from the DECT data set. Since linear correlation was shown for all SECT and almost all DECT measurements, conversion of CT numbers to estimated LFC was performed as follows:

SECT: $LFC = -155.923[\%/HU] \times SE_{120}\,[HU] + 51.685$

DECT: $LFC = -162.644[\%/HU] \times VNI\,[HU] + 52.785$

TABLE 2. CT Numbers (HU) of Contrast-Enhanced Phantoms With Different Fat and Iron Concentrations

Contrast-Enhanced Phantom	Iron Free Fat Concentration				Iron Concentration		
	0%	10%	30%	50%	1.5 mg/mL Mean Increase (95% CI)*	3 mg/mL Mean Increase (95% CI)*	6 mg/mL Mean Increase (95% CI)*
120 kV	90.1	57.9	30.9	16.1	Δ14.3 (7.8 to 20.6, $P < 0.01$)	Δ25.7 (15.4 to 35.9, $P < 0.01$))	Δ44.4 (29.2 to 59.6, $P < 0.01$)
80 kV	99.0	76.5	40.9	18.6	Δ20.2 (14.7 to 25.7, $P < 0.001$)	Δ35.1 (25.7 to 44.6, $P < 0.001$)	Δ59.9 (50.5 to 69.2, $P < 0.001$)
140 kV	74.8	57.3	27.0	8.0	Δ6.7 (2.4 to 11.0, $P < 0.05$)	Δ12.0 (4.4 to 19.5, $P < 0.05$)	Δ20.2 (−13.5 to 26.9, $P < 0.01$)
$DE_{80/140}$	88.0	62.9	34.2	13.1	Δ13.7 (5.7 to 21.8, $P < 0.01$)	Δ23.2 (13.6 to 32.8, $P < 0.01$)	Δ42.3 (34.3 to 50.2, $P < 0.001$)
DEI	−0.0052	−0.0090	−0.0067	−0.0111	Δ0.0062 (0.0052 to 0.0073, $P < 0.001$)	Δ0.0106 (0.0099 to 0.0113, $P < 0.001$)	Δ0.0179 (0.0155 to 0.0203, $P < 0.001$)
VNI	59.9	37.2	−1.7	−18.9	Δ2.1 (−3.0 to 7.1, $P = 0.27^{\dagger}$)	Δ2.4 (−4.1 to 8.9, $P = 0.33^{\dagger}$)	Δ2.7 (−2.6 to 8.0, $P = 0.20^{\dagger}$)

*Mean differences of CT numbers for iron concentrations of 1.5 mg/mL and higher compared to the mean of iron-free phantoms are shown.
†Non-significant differences.
HU indicates Houndsfield units; $DE_{80/140}$, 50%:50% linearly blended images at 80 kV and 140 kV; DEI, dual-energy index; VNI, virtual noniron images; CI, confidence interval.

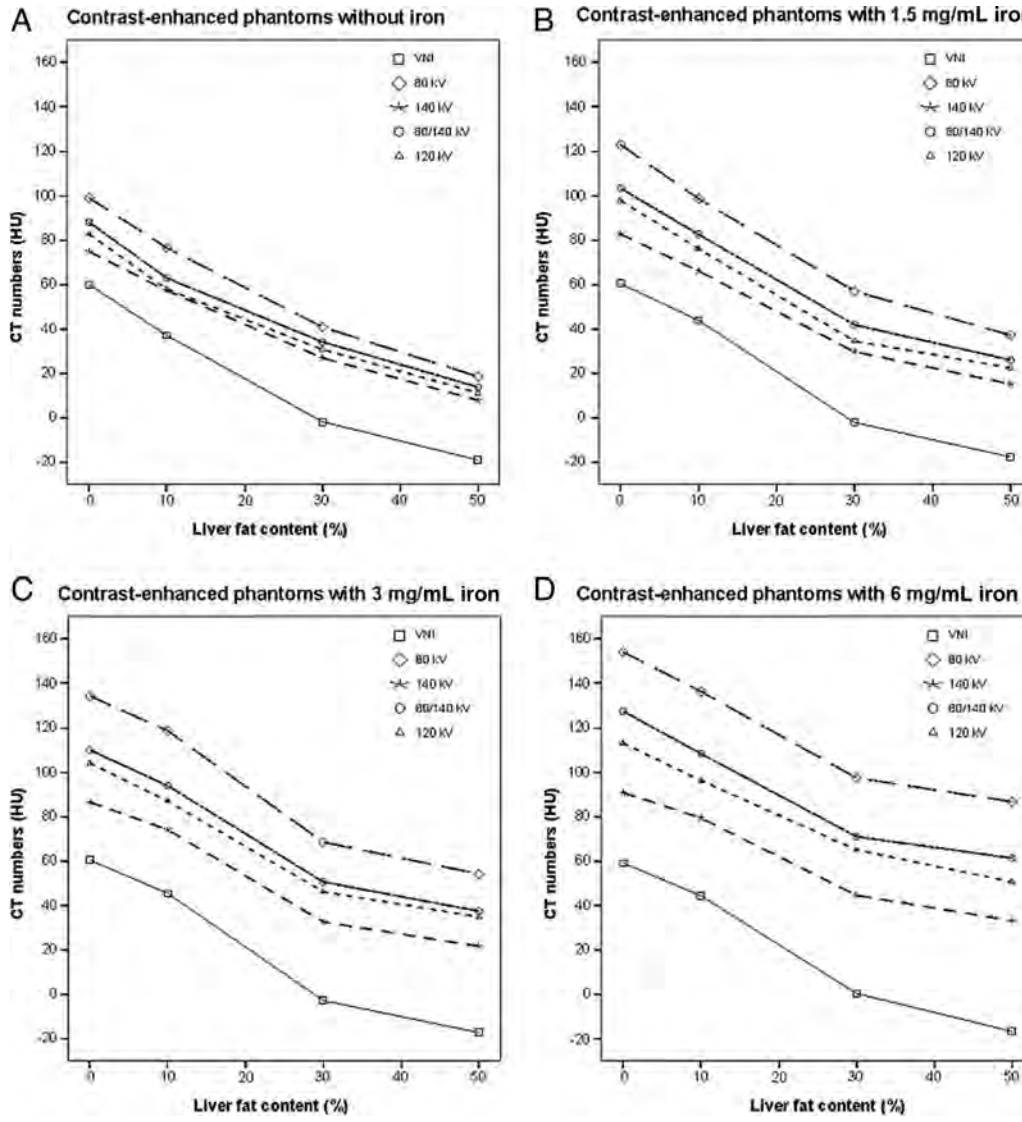

FIGURE 4. Comparison of CT numbers at 120 kV, 80 kV, 140 kV, and 80/140 kV with VNI measurements derived from DECT for contrast enhanced (iodine) phantoms with varying liver iron content (LIC). For phantoms at 0 mg/mL iron (A) both SECT and DECT measurements significantly underestimated (all, $P < 0.05$) titrated LFC, whereas VNI measurements allowed for correct LFC estimation ($P = 0.071$) being similar to "iron- and iodine- free" VNI and SECT measurements at 120 kV (Fig. 3). With increasing LIC (B–D), there was an increasing underestimation of LFC for all measurements (all, $P < 0.05$) except for VNI, which correctly estimated the LFC for low (B), medium (C) and high (D) LIC (all, $P > 0.2$).

DISCUSSION

Owing to the increasing prevalence of hepatic steatosis and its potential to progress to end-stage liver disease, accurate quantification of fat content is of major clinical interest for the primary evaluation of diffuse liver disease as well as for the monitoring of treatment response.[2–6]

SECT is known to be a useful noninvasive method for detecting and following patients with advanced stages of fatty liver diseases.[24] In clinical routine, SECT can be used for estimating the LFC, with a mean attenuation of healthy liver parenchyma ranging from 55 to 65 HU at unenhanced studies.[12] The ability of SECT for discrimination of liver tissue and fat is well reflected in our phantom study showing an excellent correlation of SECT attenuation and LFC, with a significant decline of CT numbers from 58 HU to −19.6 HU with increasing LFC from 0% to 50%, respectively.

Our results demonstrate that discrimination of liver tissue and fat is also feasible with DECT, showing an excellent correlation between CT numbers and LFC in a clinically relevant range from 0% to 50%. This is consistent with the results of a recent study showing that DECT is comparable—however not superior—to SECT for decomposition of materials with similarly low atomic numbers.[23] Thus, DECT similarly allows, but does not appear to improve, the accuracy for discriminating fat from soft tissue when compared with SECT in the nonenhanced, iron-free liver.

Storage diseases with iron, glycogen, or copper lead to an increased attenuation of the hepatic parenchyma,[12] which may confound the quantification of LFC from SECT measurements. Our results show that for elevated LIC, SECT fails to estimate the LFC due to a significant increase in CT numbers. These confounding effects of iron were present already at a low LIC of 1.5 mg/mL.

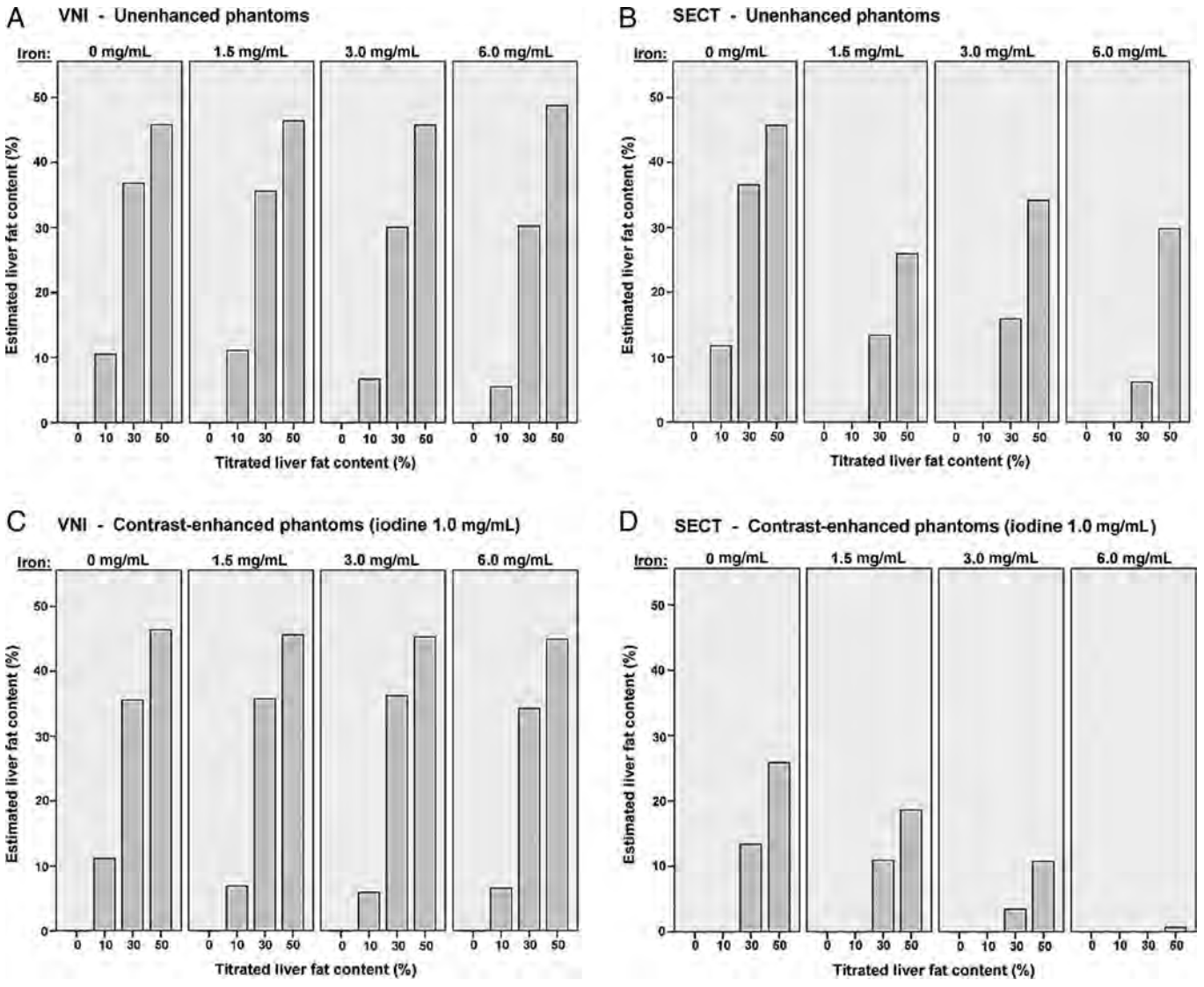

FIGURE 5. LFC quantification in the presence of 0, 1.5, 3, and 6 mg/mL iron using SECT at 120 kV and VNI from DECT at unenhanced (A, B) and contrast-enhanced scans (C, D).

Accordingly, the coexistence of iron and fat neutralize each other's effects on attenuation. For example, in our study, measurements from SECT resembled physiological liver parenchyma (59 HU) at a LIC of 3 mg/mL and a LFC of 10%. This underlines that absolute quantification of LFC is not feasible with SECT when iron is present.

DECT using low-energy data (DE_{80}) and linearly-blended low- and high-energy data ($DE_{80/140}$), as well as calculation of the DEI have previously shown promise for the identification of various soft-tissue types, calcified structures, and iodine-containing CM.[23,25] Our study indicates that DE_{80}, $DE_{80/140}$ data as well as the DEI shows no benefit over SECT for quantifying the LFC both with and without coexisting iron. This is consistent with early DECT studies showing that dual-energy images generated using different ratios of the 80 kV and 140 kV data are not helpful for detecting fatty liver infiltration in the presence of hemochromatosis or hemosiderosis.[14,26,27]

The effect of increasing LIC on CT numbers is well reflected by a parallel increase of HU values for all CT numbers, with DE_{140} representing the lower and DE_{80} the upper limit of measurements. DEI being an equation including CT numbers at both tube voltages shows the same limitations as $DE_{80/140}$, with no added value for LFC quantification.

DECT using an iron-specific 3-material decomposition algorithm, however, is able to eliminate the confounding iron from the data, allowing for the quantification of titrated LFC, regardless of the LIC. The feasibility of dual-energy 3-material decomposition was also shown for other high atomic number materials (such as iodine and bone) and thus was used to create virtual noncontrast images.[28] Iron, being a high atomic number material, shows an energy-dependent change in CT attenuation, which is inversely and linearly related to the LIC.[14] An iron-specific dual-energy 3-tissue decomposition algorithm, allowing for the subtraction of iron has, to the best of our knowledge, not been proposed before. For the reconstruction of VNI images, we performed an x-ray spectral analysis at 80 kV and 140 kV with increasing amounts of iron for optimizing the algorithm to the characteristic absorption profiles of liver tissue, fat, and iron. Using this algorithm, our results show a high accuracy for ex vivo estimation of LFC even in the presence of iron.

Our results also show that in the presence of iron and iodine, VNI images from DECT allow for the accurate quantification of titrated LFC by eliminating both iron and iodine from the data. This is most probably due to similar absorption profiles and k-edges of iron and iodine,[29] allowing the "iron-specific" algorithm to also remove iodine sufficiently. It must be noted, however, that for achieving a complete iodine subtraction from the data, the dual-energy algorithm would be needed to be adjusted to an iodine-specific slope, which would lower the accuracy of iron subtraction.

Limitations

First, we must acknowledge the inherent limitations of an ex vivo study. Thus, our results might not be transferred with the same accuracy to an in vivo setting or to other scanners.[30] Nevertheless, we used veal liver, organic fat, and an iron (Fe^{3+})-compound to mimic the in vivo components as close as possible.

Second, the calibration of the iron-specific dual-energy algorithm proposed in this study was performed with only 3 different iron concentrations and on the same phantoms used for the validation of the model, which might limit the power of our results.

Furthermore, we found strong and highly significant linear correlation between estimated LFC by CT numbers and actual LFC. Nevertheless, there are some discrepancies regarding estimation of low LFC at the presence of high iron and iodine content (6 mg/mL iron: estimated, 5.5%; actual, 10%). This may be caused by the quantification model for LFC (LFC = −162.644[%/HU] × VNI [HU] + 52.785) being based on the measurements of only 4 phantoms (containing 0%, 10%, 30%, and 50% LFC) and which might be further optimized by measurements of phantoms with lower LFC intervals.

Moreover, it is possible to measure the LIC from DECT overlay-images, which are generated next to the VNI images by the postprocessing software (Fig. 1). However, this must be the subject of further prospective studies including more than only 3 iron concentrations and evaluating the feasibility of DECT for quantification of LIC.

Finally, we did not analyze the use of a tube voltage pair of 100/140 kV, which is known to provide a better image quality for abdominal scans as compared with 80/140 kV, especially in obese patients who frequently suffer from steatosis hepatis.

CONCLUSIONS

Our ex vivo study indicates that DECT with 3-material decomposition allows for the accurate quantification of LFC even in the presence of iron and iodine. VNI images reconstructed from DECT data simulate nonenhanced SECT by eliminating iron and iodine from the images. No added value was seen for DECT as compared with SECT for LFC quantification in the absence of iron and iodine. Future studies should address the ability of DECT for fat quantification in other causes of elevated density of the liver parenchyma, such as copper in Wilson disease, gold, thallium, arsenic, glycogen, and cirrhosis.

REFERENCES

1. Farrell GC, Larter CZ. Nonalcoholic fatty liver disease: from steatosis to cirrhosis. *Hepatology*. 2006;43:S99–S112.
2. Browning JD, Szczepaniak LS, Dobbins R, et al. Prevalence of hepatic steatosis in an urban population in the United States: impact of ethnicity. *Hepatology*. 2004;40:1387–1395.
3. Clark JM, Brancati FL, Diehl AM. Nonalcoholic fatty liver disease. *Gastroenterology*. 2002;122:1649–1657.
4. Angulo P. Nonalcoholic fatty liver disease. *N Engl J Med*. 2002;346:1221–1231.
5. McCormack L, Petrowsky H, Jochum W, et al. Hepatic steatosis is a risk factor for postoperative complications after major hepatectomy—a matched case-control study. *Ann Surg*. 2007;245:923–930.
6. Nomura F, Ohnishi K, Ochiai T, et al. Obesity-related nonalcoholic fatty liver—CT features and follow-up-studies after low-calorie diet. *Radiology*. 1987;162:845–847.
7. El-Badry AM, Breitenstein S, Jochum W, et al. Assessment of hepatic steatosis by expert pathologists: the end of a gold standard. *Ann Surg*. 2009;250:691–697.
8. McGill DB, Rakela J, Zinsmeister AR, et al. A 21-year experience with major hemorrhage after percutaneous liver biopsy. *Gastroenterology*. 1990;99:1396–1400.
9. Fischer MA, Nanz D, Reiner CS, et al. Diagnostic performance and accuracy of 3-D spoiled gradient-dual-echo MRI with water- and fat-signal separation in liver-fat quantification: comparison to liver biopsy. *Invest Radiol*. 2010;45:465–470.
10. Hussain HK, Chenevert TL, Londy FJ, et al. Hepatic fat fraction: MR imaging for quantitative measurement and display—early experience. *Radiology*. 2005;237:1048–1055.
11. Sharma P, Martin DR, Pineda N, et al. Quantitative analysis of T2-correction in single-voxel magnetic resonance spectroscopy of hepatic lipid fraction. *J Magn Reson Imaging*. 2009;29:629–635.
12. Boll DT, Merkle EM. Diffuse liver disease: strategies for hepatic CT and MR imaging. *Radiographics*. 2009;29:1591–1614.
13. Hamer OW, Aguirre DA, Casola G, et al. Fatty liver: imaging patterns and pitfalls. *Radiographics*. 2006;26:1637–1653.
14. Raptopoulos V, Karellas A, Bernstein J, et al. Value of dual-energy CT in differentiating focal fatty infiltration of the liver from low-density masses. *Am J Roentgenol*. 1991;157:721–725.
15. Kohgo Y, Ohtake T, Ikuta K, et al. Dysregulation of systemic iron metabolism in alcoholic liver diseases. *J Gastroenterol Hepatol*. 2008;23(suppl 1):S78–S81.
16. Graser A, Becker CR, Staehler M, et al. Single-phase dual-energy CT allows for characterization of renal masses as benign or malignant. *Invest Radiol*. 2010;45:399–405.
17. Goldberg HI, Cann CE, Moss AA, et al. Noninvasive quantitation of liver iron in dogs with hemochromatosis using dual-energy CT scanning. *Invest Radiol*. 1982;17:375–380.
18. Stolzmann P, Leschka S, Scheffel H, et al. Characterization of urinary stones with dual-energy CT: improved differentiation using a tin filter. *Invest Radiol*. 2010;45:1–6.
19. Thomas C, Krauss B, Ketelsen D, et al. Differentiation of urinary calculi with dual energy CT: effect of spectral shaping by high energy tin filtration. *Invest Radiol*. 2010;45:393–398.
20. Tavill AS. Diagnosis and management of hemochromatosis. *Hepatology*. 2001;33:1321–1328.
21. Olivieri NF, Saxon BR, Nisbet-Brown E, et al. Quantitative assessment of tissue iron in patients (pts) with sickle cell disease. *Blood*. 1997;90(Suppl. 1):1976.
22. Liu X, Yu L, Primak AN, et al. Quantitative imaging of element composition and mass fraction using dual-energy CT: three-material decomposition. *Med Phys*. 2009;36:1602–1609.
23. Zachrisson H, Engstrom E, Engvall J, et al. Soft tissue discrimination ex vivo by dual energy computed tomography. *Eur J Radiol*. 2010;75:e124–e128.
24. Bydder GM, Chapman RW, Harry D, et al. Computed-tomography attenuation values in fatty liver. *J Comput Tomogr*. 1981;5:33–35.
25. Robinson E, Babb J, Chandarana H, et al. Dual source dual energy MDCT: comparison of 80 kVp and weighted average 120 kVp data for conspicuity of hypo-vascular liver metastases. *Invest Radiol*. 2010;45:413–418.
26. Mendler MH, Bouillet P, Le Sidaner A, et al. Dual-energy CT in the diagnosis and quantification of fatty liver: limited clinical value in comparison to ultrasound scan and single-energy CT, with special reference to iron overload. *J Hepatol*. 1998;28:785–794.
27. Oelckers S, Graeff W. In situ measurement of iron overload in liver tissue by dual-energy methods. *Phys Med Biol*. 1996;41:1149–1165.
28. Scheffel H, Stolzmann P, Frauenfelder T, et al. Dual-energy contrast-enhanced computed tomography for the detection of urinary stone disease. *Invest Radiol*. 2007;42:823–829.
29. Johnson TR, Krauss B, Sedlmair M, et al. Material differentiation by dual energy CT: initial experience. *Eur Radiol*. 2007;17:1510–1517.
30. Levi C, Gray JE, Mccullough EC, et al. The unreliability of CT-numbers as absolute values. *Am J Roentgenol*. 1982;139:443–447.